Nd:YAG Laser Processing of Thick NiTi Wires to Locally Alter Transformation Properties Towards Achieving Multiple Memory Shape Memory Alloys

Amin Alipour, Mahmoud Kadkhodaei*, Ehsan Foroozmehr

Department of Mechanical Engineering,
Isfahan University of Technology, Isfahan 8415683111, Iran
E-mail: alipoor68@gmail.com, kadkhodaei@iut.ac.ir, eforoozmehr@iut.ac.ir
*Corresponding author

Abstract: Every commercial NiTi (Nitinol) Shape Memory Alloy (SMA) has its own transformation temperatures, which may cause limitations in ever-growing demands for the application of these alloys in novel engineering designs. Among various methods proposed to achieve multiple functional characteristics, laser processing offers effective solutions in locally controlling the transformation properties of NiTi parts. The current work describes the application of laser technique followed by post-processing to locally alter transformation temperatures and impose phase transition for thick NiTi wires. To this end, various laser parameters are applied, and the influences of peak power and pulse width on the functional, microstructural, and mechanical properties of laser processed samples are studied. A four-sided laser processing protocol is proposed to process almost the whole cross section of thick Nitinol wires. It is also shown that post-processing heat treatment is required to recover the shape memory properties of as-processed Nitinol specimens. The transformation temperatures of the final processed Nitinol wire increase by about 50 °C compared to those of the unprocessed base material.

Keywords: Multiple Memory Shape Memory Alloy, Nd:YAG Laser, Post-Processing

Research paper

1   INTRODUCTION

The unique responses of Shape Memory Alloys (SMAs), including Shape Memory Effect (SME) and Pseudoelasticity (PE), make them an ideal option to be widely applied in various high tech. industries. SME is the ability to eliminate the residual strains after the loading cycle upon heating whereas, based on the PE effect, a large amount of strains can be spontaneously recovered through a mechanical loading/unloading cycle. Due to better strength, corrosion resistance, ductility, stability of transformation temperatures, and biocompatibility, NiTi is the most well-known and applicable shape memory alloy [1]. The extraordinary features of SME and PE depend on the composition and processing history of Nitinol alloys [1-2]. Since these characteristics are uniform through commercial NiTi elements, they pose only one set of transformation properties leading to the so-called single memory SMAs. However, new engineering demands urge promoting functionality and enhancing design adjustability of applied components. One way to address this issue is embedding more transformation properties by locally controlling the microstructure and/or composition of NiTi-based SMAs. Consequently, various approaches have been so far proposed to locally tune the properties of monolithic Nitinol alloys.

As one of the first attempts, Miura et al. [3] used different Direct Electric Resistance Heat Treatment (DERHT) for each section of an orthodontic wire. Hence, each section experienced a distinct processing history and, consequently, achieved varying transformation properties. Gradient annealing of SMA wires using tube furnace [4], joining of dissimilar SMA wires [5], inducing gradient heat treatment over an SMA wire by Joule Heating [6], establishment of a triple-SME applying R-phase [7], applying geometric gradient [8-12], and compositionally grading NiTi plates via surface diffusion of Ni through the plate thickness [13] can be mentioned as the reported attempts to enhance the functional properties of NiTi SMAs. Khan [14] introduced a laser induced controlled vaporization technique to manage the transformation temperatures of SMAs. Employing the high power density of an Nd:YAG laser, they could impart variations in the alloy's chemical composition resulting from the preferential vaporization of Nickel. Moreover, they studied the influences of laser parameters (pulse time, peak power, and the number of pulses per spot) on microstructure, transformation temperatures, and mechanical properties of laser-processed monolithic sheets [14]. This technique was utilized to produce various multiple memory NiTi-based devices [15-18]

Although NiTi based SMAs are vastly utilized in various smart structures in the form of wire or ribbon, major investigations on laser processing have been concentrated on sheets [1-2], [19-21]. There are limited works dedicated to study the processing of NiTi in the form of wires. As one of these attempts, Michael [22] applied pulsed Nd:YAG laser to process Nitinol wires. They focused on the superior vaporization of Ni in the course of laser processing and developed a model to predict changes in Ni concentration of the processed samples in terms of peak power and laser pulse duration. Moreover, Panton [23] studied the thermomechanical fatigue properties of NiTi laser welded joints. To this end, a NiTi wire containing a single laser-processed spot was investigated. They also explored the characterization of laser-processed NiTi wires. Based on their analysis results, a thermomechanical treatment was presented to enhance the properties of the products. Additionally, Pequegnat [24] investigated the use of pulsed Nd:YAG laser processing accompanying post-processing to adjust the local SME as well as PE properties of uniform NiTi wires. They utilized this technique to induce various memories in a desired section of a monolithic NiTi linear actuator. Deformation of the product was further characterized and compared with that of a single memory actuator. In another part of their work, microstructure and composition of the processed material were determined to uncover the influences of laser processing accompanied by cold working and heat treatment. Besides laser processing, there are several works regarding the effects of laser welding on the shape memory properties of Nitinol wires [25-28].

All the wires applied in the previous studies [22-24] were very thin with a diameter no bigger than 700 μm, commonly used for medical devices. However, for thicker NiTi wires, the energy required to process the wire as well as laser processing conditions would change. Although only one-sided laser processing was considered and studied in previous works, due to the small sizes of wires, more than one-side processing may be required to reach almost full penetration in rather thick wires. Therefore, distinct investigations are required to study the laser processing of such thick Nitinol wires.

The current research is dedicated to the utilization of Nd:YAG laser processing together with post heat treatment to alter local transformation temperatures and induce phase conversion in thick NiTi wires. To this end, various laser parameters are examined on a relatively thick Nitinol wire, and the thermal, microstructural, and compositional properties of the processed samples are investigated via characterization analyses. The effects of pulse width and peak power are investigated in order to impart changes in the transformation properties of the monolithic NiTi wire and induce phase transition. A four-sided laser processing pattern is presented to fully penetrate into the whole cross-section of the wire. Then, annealing is applied to recover the shape memory

property of the as-processed specimen. Finally, a laser-processed NiTi wire is successfully produced with new transformation temperatures so that the product shows SME at room temperature, unlike the as-received base material which exhibits PE properties.

2   MATERIALS AND METHODS

A 1.35 mm diameter Nitinol wire manufactured by Small Parts; Inc. was employed in this study. The samples were treated by the provider to exhibit pseudoelasticity at room temperature. The nominal chemical composition of the purchased alloy was 49.3 at. % (44.2 wt.%) Ti and 50.7 at. % (55.8 wt.%) Ni. The wires were cut into 60 mm length samples, and only 35 mm of the central length of each sample was laser processed. To eliminate a dark oxide layer developed during the process, the wires were acid pickled in a solution containing HNO_3, HF, and H_2O with volume percentages of 20%, 7.5%, and 72.5%, respectively, for 40 seconds before the laser processing. Then, any probably remaining contaminants were removed by cleaning the wires with Ethanol and de-ionized water.

A 400 W pulsed Nd:YAG laser system with a wavelength of 1.06 μm, a nominal spot diameter of 1.3 mm, and a square profile was utilized. The laser power was measured by a Gentec-EO pronto-500 power meter. As illustrated in "Fig. 1", the Nitinol wires were relied on a flat base plate, and two clamps held down their both ends to avoid any movement during laser processing.
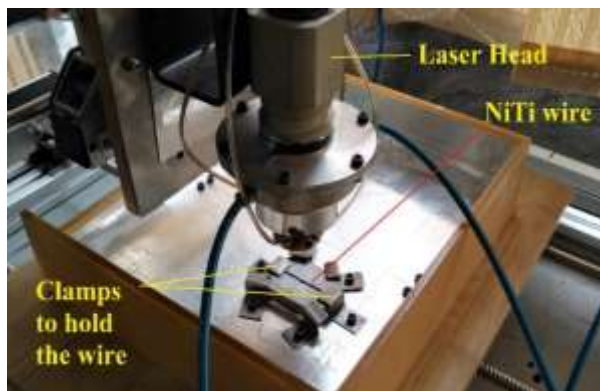

Fig. 1   Laser setup.

A 3-axis CNC machine provided controlled movement of the NiTi wires while the laser processing was done. The laser spots were overlapped by 60% to optimize the surface finish in the course of removing a brittle terminal solidification region. The wire was surrounded by a plastic chamber according to "Fig. 2". This chamber, filled with argon at the onset of laser processing, shielded the wire to minimize oxidation during the

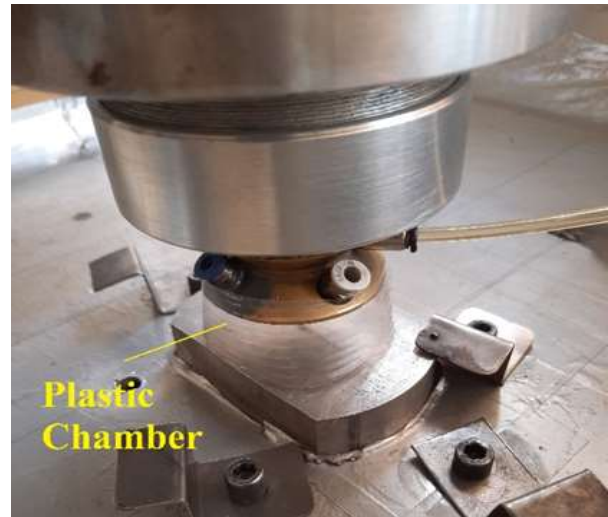process. The flow rate of 10 lit/min for Argon shielding gas was found enough to avoid oxidation.

Fig. 2   Plastic chamber designed to avoid oxidation.

Differential Scanning Calorimetry (DSC) analysis at a controlled heating and cooling rate of 5°C/min was performed using a Mettler Toledo, DSC1 system equipped with a Refrigerated Cooling System (RCS). The chemical composition of the processed specimens was determined using EDAX Octane Elite system equipped with FEI Quanta 450 microscope. Santam universal testing machine model STM 50 equipped with a thermal chamber was employed to evaluate deformations of the as-received and the laser-processed wires. Tensile samples had a gauge length of 35 mm and were loaded at a strain rate of 1.5×10^{-3} 1/s. The Effects of strain rate for a special kind of SMA [29] and gauge geometry in tensile test [30] were investigated previously. Tensile tests were carried out at the ambient temperature (25 °C). In order to investigate the microstructure of the processed specimens, metallographic samples were cross-sectioned, cold mounted in epoxy, and mechanically polished. Prior to mechanical polishing with colloidal alumina suspension, grinding with sequential sand paper of 400 to 1200-fine grit was performed. Finally, to reveal their microstructure, the samples were etched in a 3 mL HF, 14 mL HNO_3, and 82 mL H_2O solution for about 30 s.

3   RESULTS AND DISCUSSION

To investigate the influence of laser processing on the transformation temperatures of the NiTi specimens, first, the unprocessed base Nitinol wire was needed to be characterized. Figure 3a shows the DSC results for the as-received material.
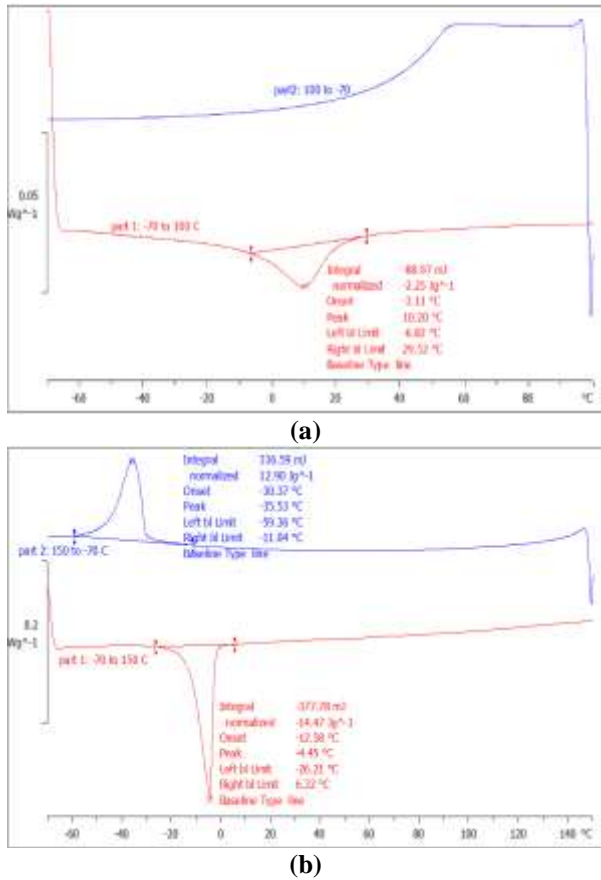
(a)

(b)

Fig. 3   DSC results for: (a): as-received material, and
(b): HBM.

Table 1 Critical temperatures of HBM

Sample	Transformation and Peak Temperatures, °C					
	M_f	M_s	A_s	A_f	M_p	A_p
HBM	- 59.4	- 11	- 26.2	6.3	- 35.5	- 4.5

Due to thermomechanical processes in the course of wire fabrication, broad temperature peaks occur in the cooling cycle that do not allow for identifying the transformation temperatures. To remove such effects and to suppress the possible formation of R-phase, the as-received NiTi wire was heat treated at 800 °C for 1 hour followed by water quenching [1]. This heat-treated base material is referred to as HBM in the rest of this study. The DSC curves for HBM are plotted in "Fig. 3b". As observed, intense DSC peaks are obtained for HBM so the critical temperatures can be easily measured. These critical temperatures for HBM are listed in "Table 1" and are considered as the reference temperatures for the rest of the work. Referring to an SMA phase diagram [31], M_s, M_f, A_s and A_f are transformation temperatures and respectively represent the onset and the end of

forward and reverse transformations in stress-free conditions.

Since these transformation temperatures depend on how the tangents to the DSC curves are taken, two other parameters as the peaks of forward and reverse martensitic transformation temperatures are also considered for comparative analyses. These two parameters, known as martensite peak temperature (M_p) and austenite peak temperature (A_p), can be derived by the DSC graphs where the first derivative is zero and are more reliable for comparison purposes.

Inspired by the laser parameters used in previous analyses for sheets and thin wires [14], [22-24], two initial sets of laser parameters are defined according to "Table 2". The Nitinol wires processed by these laser parameters are referred to as LP 1 and LP 2, respectively. As shown in "Table 2", a 10 ms pulse width with a 10 1/s frequency is similarly used for both parameter sets. However, two amounts of 1 kW and 1.2 kW are respectively applied as the peak power for LP 1 and LP 2. It is worth mentioning that these amounts of peak power are the highest ones that can be applied to preserve the material integrity for these certain values of pulse width and frequency.

Table 2 Two initial sets of laser parameters

Sample	Laser Parameters		
	Pulse width, ms	Peak Power, kW	Frequency, 1/s
LP 1	10	1	10
LP 2	10	1.2	10

To analyze the influence of laser processing with mentioned parameters on the transformation temperatures, a DSC test was conducted for LP 1 as well as LP 2 samples. The DSC results are illustrated in "Fig. 4", and the corresponding critical temperatures are summarized in "Table 3". By comparing the data of "Table 3" and "Table 1", it can be inferred that the laser processing has not affected the critical temperatures, especially the transformation peak temperatures, of LP 1 and LP 2 compared to those of the reference HBM sample. It has been shown that the composition change is the primary mechanism responsible for the alteration of SMA transformation properties via laser processing [1]. The high energy density of the laser can induce vaporization in SMA elements. Due to the larger vapor pressure of Nickel compared to that of Titanium, more Nickel vaporizes during laser processing resulting in a composition change in the material. Hence, no change in the transformation temperatures of LP 1 and LP 2 can be due to insufficient power provided by these laser parameters which cannot raise the temperature highly enough for element vaporization and composition change.
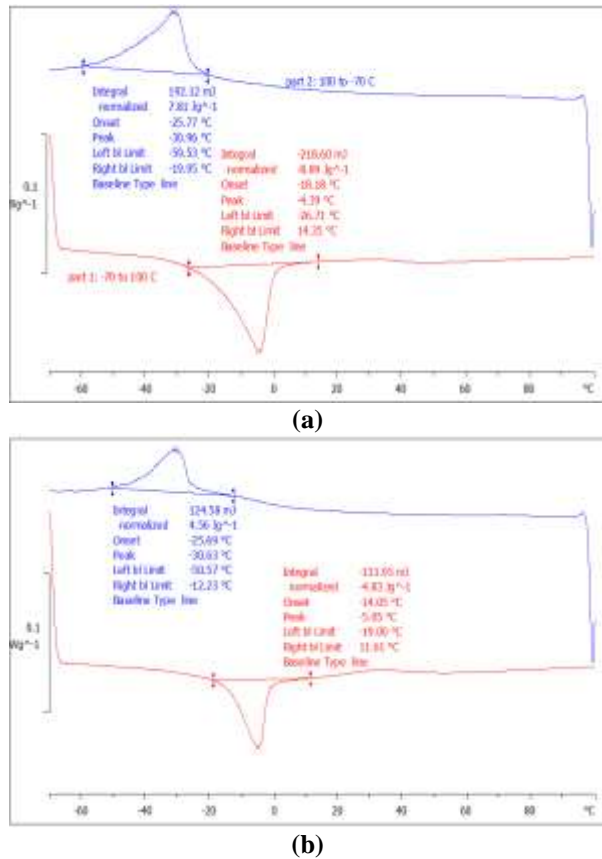
(a)

(b)

Fig. 4   DSC results for: (a): LP 1, and (b): LP 2.

Table 3 Critical temperatures of LP 1 and LP 2

	Transformation and Peak Temperatures, °C					
Sample	M_f	M_s	A_s	A_f	M_p	A_p
LP 1	- 59.5	- 20	- 26.7	14.4	- 31	- 4.4
LP 2	- 50.6	- 12.2	- 19	11.6	- 30.6	- 5.1

Table 4 Second sets of laser parameters

	Laser Parameters		
Sample	Pulse width, ms	Peak Power, kW	Frequency, 1/s
LP 3	7	1.5	10
LP 4	8	1.5	10

Relative changes in material composition during laser processing mostly depend on a balance between the dilution of the molten pool and the vaporization flux of alloy elements [32-33]. Since these two issues are strongly associated with laser processing parameters [1], it is essential to study the effects of both pulse duration and peak power, as the key laser parameters, on the resultant transformation temperatures.

To investigate the effect of higher peak power, the amount of peak power was increased, and two new sets

of processing conditions as LP 3 and LP 4 were defined according to "Table 4".

In contrast, the amount of pulse width was decreased slightly to avoid any breakage of the wire while processing. The samples LP 3 and LP 4 were subjected to DSC analysis, and the results are shown in "Fig. 5".
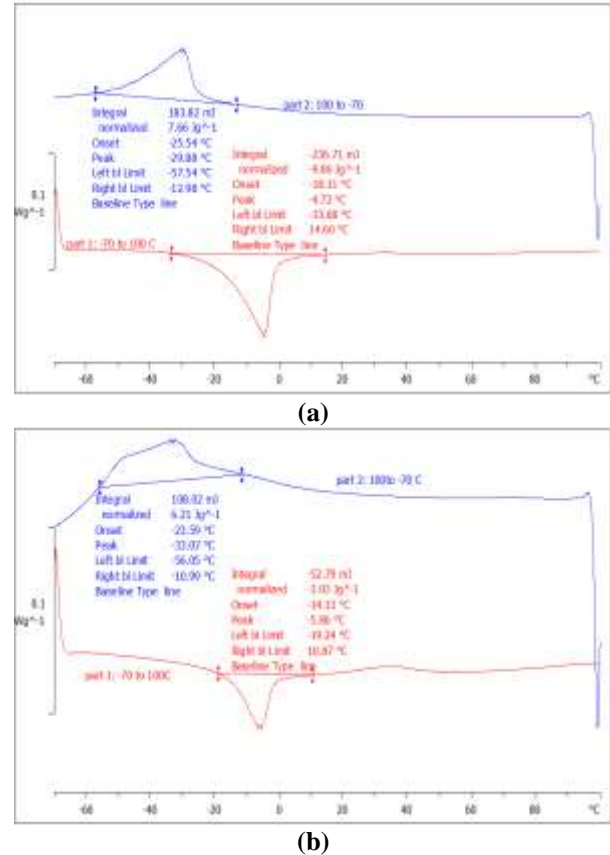

(a)

(b)

Fig. 5   DSC results for: (a): LP 3, and (b): LP 4.

The critical temperatures are extracted and reported in "Table 5". As noted, the transformation temperatures of the newly processed wires do not considerably vary compared to the reference temperatures. In depth comparison of transformation temperatures showed that, while M_f and M_s temperatures were almost the same as the reference temperatures, A_s showed a different approach for each of the two processed samples, and A_f showed a slight increase for both cases. As mentioned above, this inconsistency is attributed to the method of deriving the transformation temperatures and depends on how the tangents to the DSC graphs are taken. However, the transformation peak temperatures for HBM, LP 3, and LP 4 are closer than the one observed for the transformation temperatures, especially much closer for A_p values, which presents a difference of less than 2 °C. Consequently, all the transformation temperatures can be considered unchanged compared to the reference ones.

Table 5 Critical temperatures of LP 3 and LP 4

Sample	Transformation and Peak Temperatures, °C					
	M_f	M_s	A_s	A_f	M_p	A_p
LP 3	- 57.5	- 13	- 33.7	14.6	- 29.9	- 4.7
LP 4	- 56	- 11	- 19.2	10.8	- 33.1	- 5.9

The effect of higher pulse width, as another key parameter of laser processing, can be studied in the next step. Additionally, referring to a map of laser profiles presented by Michael [22], as seen in "Fig. 6", it is suggested that a longer pulse width results in better penetration while preserving the material integrity.
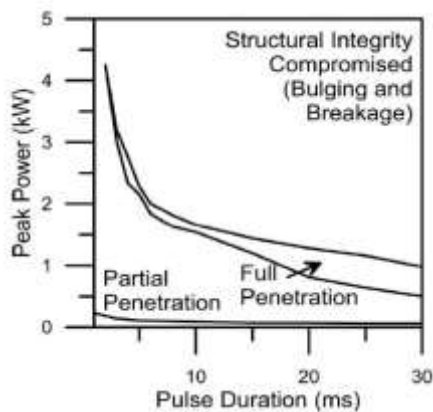

Fig. 6 The curve for penetration conditions according to the amount of peak power and pulse duration [22].
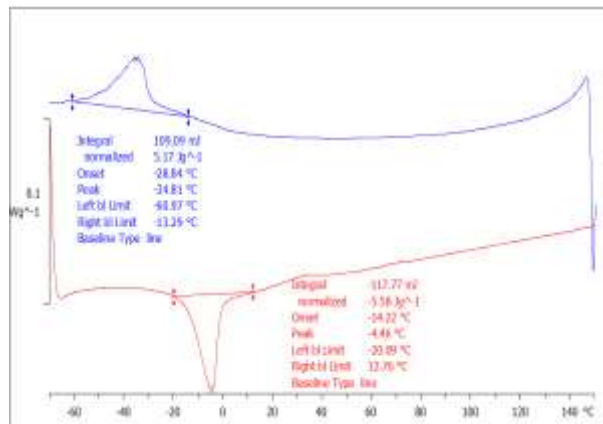

Fig. 7 DSC results for LP 5.

To this end, a new set of laser parameters with higher pulse width is introduced. This new set has a pulse duration of 20 ms, and a peak power of 0.5 kW with a 10 1/s frequency, which is referred to as LP 5 in the remainder of this study. It is worth mentioning that the amount of peak power adopted for this processing condition is lower than the one suggested by Michael map [22] ("Fig. 6"). However, it was observed that, for a 20 ms pulse width, the peak power of 0.5 kW is the

highest value that preserves the material integrity of the current NiTi wire. Thermal analysis was carried out for the LP 5 specimen, and the DSC curve is exhibited in "Fig. 7".

The corresponding critical temperatures are derived and listed in "Table 6". Once more, it can be noted that the critical temperatures, especially the transformation peak temperatures, of the new sample LP 5 have almost not varied compared to the reference ones. This is in good agreement with previous empirical results [1] and is because of the fact that vaporization occurs during the initial instances of laser processing and significantly decreases by increasing the pulse time [1]. Therefore, while the vaporization flux decreases, the volume of the molten pool increases by increasing pulse width resulting in small changes in the transformation temperatures of Nitinol wires.

Table 6 Critical temperatures of LP 5

Sample	Transformation and Peak Temperatures, °C					
	M_f	M_s	A_s	A_f	M_p	A_p
LP 5	- 61	- 13.3	- 20.1	12.8	- 34.8	- 4.5

To investigate whether such laser processing is capable of vaporizing the alloy elements and changing its composition, LP 5 sample is subjected to EDX analysis. As shown in "Fig. 8", EDX scan analysis was performed across a surface line including both the processed and the unprocessed parts of the sample. According to this figure, Nickel reduction can be detected whereas the average unprocessed Nickel content (55.8 wt.%) was significantly higher than that of the processed section of Nitinol wire. Thus, compositional analysis results confirmed that preferential Ni vaporization occurred due to laser processing. However, since EDX analysis was performed on the outer surface of the specimen, to examine the depth of these composition changes and to uncover the laser penetration, the cross-section of the processed wire must be microstructurally studied.
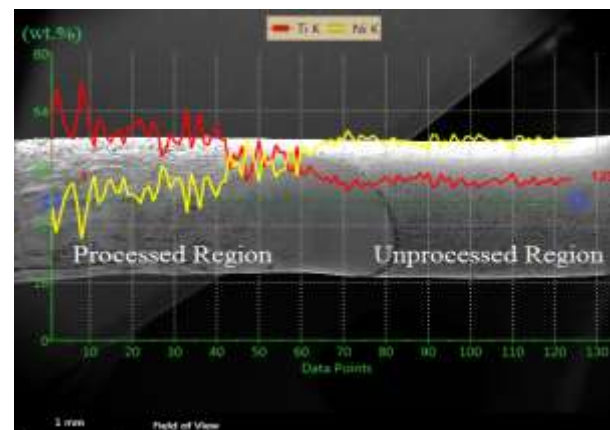

Fig. 8 EDX line scan across unprocessed and processed regions of LP 5.

The metallographic examination was conducted on the cross section of LP 5 specimen to better recognize the effect of laser processing on the microstructure and the amount of laser penetration through the thickness of NiTi wire. Optical micrographs showing the cross section of the processed wire after etching are provided in "Fig. 9".
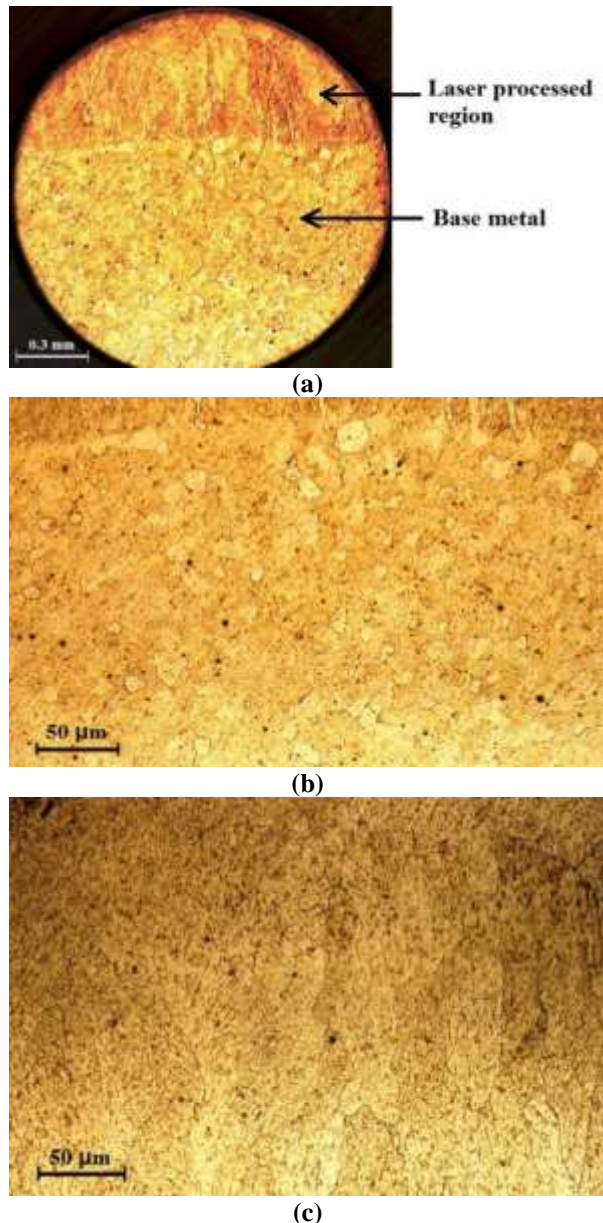

(a)

(b)

(c)

Fig. 9   Microstructure of cross-sectioned LP 5 sample: (a): whole cross section, (b): magnified image of the base metal, and (c): magnified image of the laser processed region.

According to "Fig. 9a", the wire cross section can be divided into two distinct parts. Referring to higher optical magnification of each part, "Fig. 9b" and c, it can be concluded that the main part of the wire shows an equiaxed B2 austenite grain structure which is attributed

to unprocessed base material. However, the upper part of the wire exposed to laser spot shows columnar dendritic microstructure, which is typical for processed NiTi wires [24]. Therefore, the laser beam can only process the smaller section of such thick Nitinol wires and the larger part remains unprocessed.

It is worth mentioning that, to cover the whole surface of the wire by laser spot, the spot diameter must be approximately the same as the wire diameter. Due to the relatively large sizes of the wires in the current study, the laser spot diameter (1.3 mm) is at least two times greater than the maximum spot diameter (600 μm) employed for processing thin NiTi wires [22-24]. Since the amount of laser energy applied in the present work is relatively in the same order as those for thin wires, the efficient energy density decreases to at least one-quarter. The low energy density of the laser beam leads to the fact that full penetration cannot be attained in the case of thick NiTi wires by only one-sided laser processing.

To overcome this challenge, a four-sided laser processing technique is proposed to process almost the entire thick NiTi wires and can alter transformation properties compared to those of the reference sample. According to this approach, the laser is irradiated in four equally angel sides of the wire. When the processing of one side has been completed, the wire is rotated by 90 degrees and the new side is processed. This procedure is repeated for each of the four sides of the wire. The four-sided laser-processed NiTi wire, which has the same laser parameters as LP 5 sample, is called LP 6 in the rest of the work. Thermal analysis reveals that DSC peaks of LP 6 become shallow and wide, as depicted in "Fig. 10".
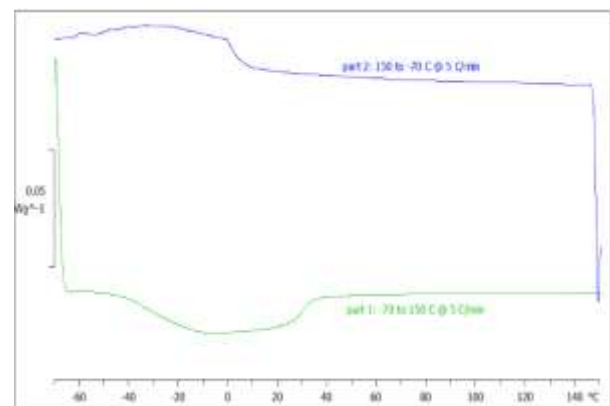

Fig. 10   DSC results for LP 6.

In other words, the laser processing caused the shape memory properties of LP 6 to be weakened. This may be attributed to rapid solidification of the molten metal after laser processing. This event can lead to inhomogeneity through the fusion zone, which is itself because of micro segregation of the alloy's elements while the solidification front is growing [23]. Due to this

inhomogeneity, internal strain/stress fields form in the alloy. These internal fields prevent the mobility of the crystals in the course of the heating and cooling cycles [34] and can even suppress the phase transition. Moreover, LP 6 sample becomes very brittle and can be easily broken when imposed to smooth bending. This brittleness may be attributed to the creation of brittle intermetallic compounds including Ti2Ni [14].

Taking all of the above into consideration, it can be inferred that a thermomechanical treatment needs to be employed to recover the shape memory effect and the ductility of the processed specimen. Annealing at 1000 °C for 1 hour followed by slow furnace cooling was found to be the best option to address all the aforementioned issues. The annealing treatment at this temperature eliminates the internal strain/stress fields from the material, improves material ductility, and also homogenizes the microstructure. The LP 6 sample which is heat treated according to the aforementioned pattern is referred to as HLP 6.

The DSC curve for HLP 6 is plotted in "Fig. 11". As illustrated, annealing heat treatment decreases the width of the transformation peaks and recovers the shape memory properties of the specimen. The critical temperatures are extracted and listed in "Table 7".
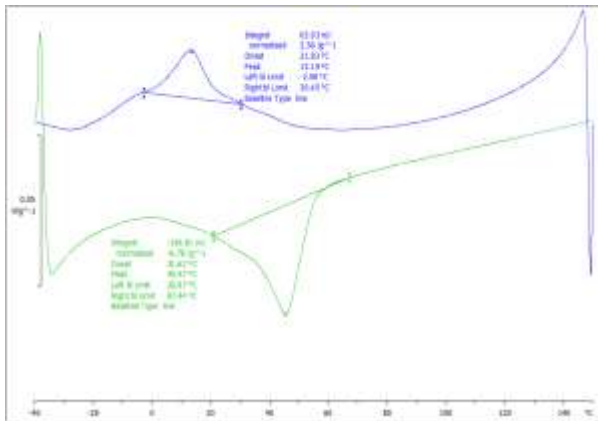

Fig. 11 DSC results for HLP 6.

Table 7 Critical temperatures of HLP 6

Sample	Transformation and Peak Temperatures, °C					
	M_f	M_s	A_s	A_f	M_p	A_p
HLP 6	- 3	30.5	20.9	67.4	13.2	45.5

Recalling reference temperatures in "Table 1", it can be noticed that the transformation peak temperatures of HLP 6 increase by about 50 °C compared to those of HBM sample. The transformation temperatures, showing scattered data, increase by a range of 40 – 60 °C compared to the reference ones. Consequently, an almost constant increase of 50 °C, can be considered for all the transformation temperatures. This confirms the successful application of Nd:YAG laser processing accompanied by post-heat treatment to alter the transformation temperatures of the thick NiTi wire. Although the base material exhibits PE at room temperature, 50 °C increase in the transformation temperatures causes a phase conversion in HLP 6 specimen so that it shows SME at room temperature.
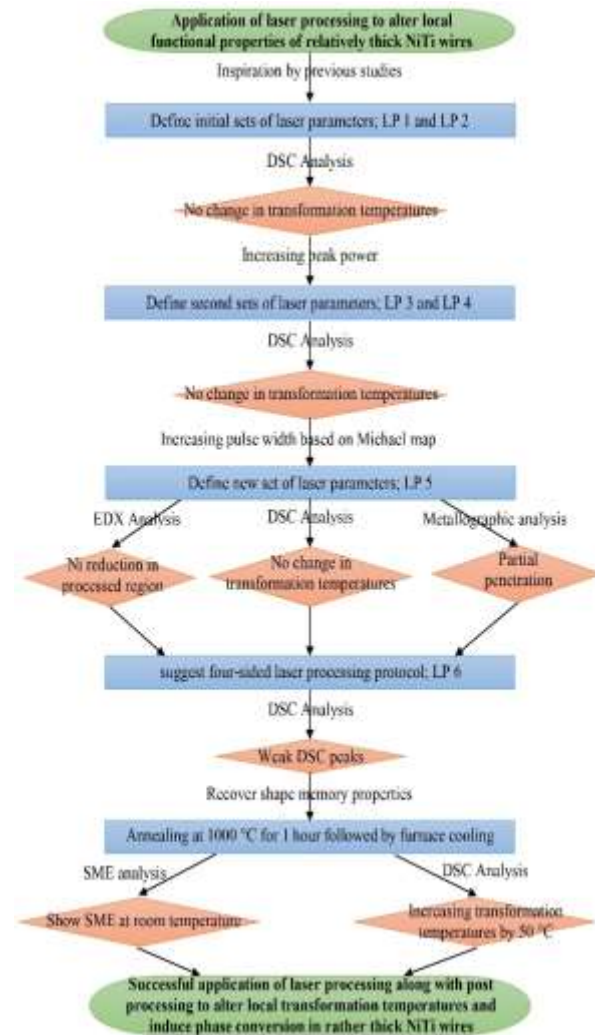

Fig. 12 A flowchart schematically detailing the procedure of altering the transformation properties of thick NiTi wires.

This can be verified by simply bending the HLP 6 to induce a small amount of residual strain and then heating it above A_f. The bent wire recovers almost all the residual strains and regains its initial straight condition upon heating. Hence, the four-sided laser processing protocol can locally alter the transformation temperatures, which can be applied to impart additional memories into a monolithic NiTi wire and to produce multiple memory materials. The corresponding

flowchart, which schematically details the procedure of altering the transformation properties of thick NiTi wires, is shown in "Fig. 12". To study the influence of laser processing on mechanical properties of NiTi samples, tensile tests were carried out for both HLP 6 and HBM, and the results are compared in "Fig. 13".
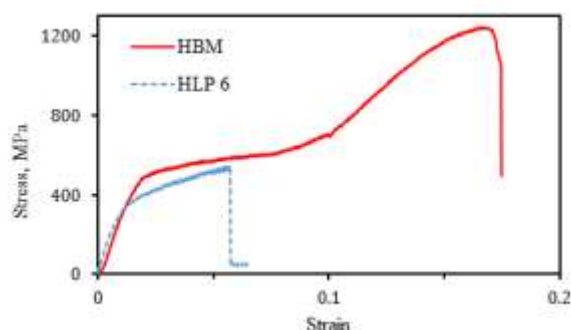

Fig. 13   Stress-strain curves for HBM and HLP 6 samples.

As depicted, the ultimate tensile stress and strain decreased significantly for HLP 6 compared to those of HBM. This reduction can be attributed to several factors including dislocation destruction, grain growth [2], segregation of solute in the course of solidification, and dendritic structure [14] in the processed metal. However, the strength and other mechanical features of the processed wire may be improved by cold working such as wire drawing.

It is worth mentioning that, the critical stress to form the stress induced martensite for HLP 6 is lower than that of HBM. This is consistent with increasing in transformation temperatures of the laser processed specimen. Referring to an SMA phase diagram [31], higher transformation temperatures lead to lower critical stresses required for phase transition to stress-induced martensite at a specific temperature.

4   CONCLUSIONS

Nd:YAG laser processing followed by post-processing heat treatment is successfully applied in current study to alter local functional properties of relatively thick NiTi wires. To this end, various laser parameters are applied, and the effects of pulse width and peak power are studied. DSC results reveal that no transformation temperature variations occur in one-sided laser processed thick wires. Further EDS analyses confirmed that preferential Nickel vaporization occurred in the processed region of the NiTi wire. However, based on metallographic results, laser beam processed a small part of cross section of the wire whereas these laser parameters provide the maximum input energy while preserving the structural integrity of the wire. It can be

concluded that one-sided laser processing cannot affect the transformation temperatures of such thick NiTi wires because of the low energy density of the laser beam. To address this issue, a four-sided laser processing technique is presented which processes the four equal-angle sides of the wire.

After such four-sided processing, however, the shape memory properties weaken due to the generation of internal strains/stresses as a result of rapid solidification after laser processing. Post-processing annealing treatment at 1000 °C followed by furnace cooling was applied to recover the shape memory properties and ductility of the processed specimen. Finally, a heat-treated laser-processed NiTi wire was produced with 50 °C higher transformation temperatures and stable martensite phase at room temperature. Deformation of the processed wire reveals that the strength and ductility decrease considerably compared to the unprocessed base material. It shows that, despite unique advantages, laser processing has several detrimental influences including dislocation destruction, grain growth, and solute segregation that lead to a lower mechanical strength. The present work proposes an approach to produce multiple shape memory effects in thick NiTi wires.

REFERENCES

[1]   Khan, M. I., Pequegnat, A., and Zhou, Y. N., Multiple Memory Shape Memory Alloys, Advanced Engineering Materials, Vol. 15, No. 5, 2013, pp. 386-393.

[2]   Pequegnat, A., Panton, B., Zhou, Y. N., and Khan, M. I., Local Composition and Microstructure Control for Multiple Pseudoelastic Plateau and Hybrid Self-Biasing Shape Memory Alloys, Materials and Design, Vol. 92, 2016, pp. 802-813.

[3]   Miura, F., Mogi, M., and Ohura, Y., Japanese NiTi Alloy Wire: Use of The Direct Electric Resistance Heat Treatment Method, The European Journal of Orthodontics, Vol. 10, No. 1, 1988, pp. 187-191.

[4]   Mahmud, A. S., Liu, Y., and Nam, T. H., Design of Functionally Graded NiTi by Heat Treatment, Physica Scripta, T129, 2007, pp. 222.

[5]   Sevilla, P., Martorell, F., Libenson, C., Planell, J. A., and Gil, F. J., Laser Welding of NiTi Orthodontic Archwires for Selective Force Application, Journal of Materials Science: Materials in Medicine, Vol. 19, 2008, pp. 525-529.

[6]   Kang, S. W., Cho, G. B., Yang, S. Y., Liu, Y., Yang, H., Miyazaki, S., and Nam, T. H., Transformation Temperatures and Shape Memory Characteristics of a Ti–45Ni–5Cu (at%) Alloy Annealed by Joule Heating, Physica Scripta, T139, 2010, pp. 014068.

[7]   Tang, C., Huang, W. M., Wang, C. C., and Purnawali, H., The Triple-Shape Memory Effect in NiTi Shape

Memory Alloys, Smart Materials and Structures, Vol. 21, No. 8, 2012, pp. 085022.

[8] Shariat, B. S., Liu, Y., and Rio, G., Mathematical Modelling of Pseudoelastic Behaviour of Tapered NiTi Bars, Journal of Alloys and Compounds, Vol. 577, 2013, pp. 76-82.

[9] Shariat, B. S., Liu, Y., and Rio, G., Modelling and Experimental Investigation of Geometrically Graded NiTi Shape Memory Alloys, Smart Materials and Structures, Vol. 22, No. 2, 2013, pp. 025030.

[10] Shariat, B. S., Liu, Y., and Bakhtiari, S., Modelling and Experimental Investigation of Geometrically Graded Shape Memory Alloys with Parallel Design Configuration, Journal of Alloys and Compounds, Vol. 791, 2019, pp. 711-721.

[11] Shariat, B. S., Bakhtiari, S., Yang, H., ansd Liu, Y., Computational and Experimental Analyses of Martensitic Transformation Propagation in Shape Memory Alloys, Journal of Alloys and Compounds, Vol. 806, 2019, pp. 1522-1528.

[12] Shariat, B. S., Bakhtiari, S., Yang, H., and Liu, Y., Controlled Initiation and Propagation of Stress-Induced Martensitic Transformation in Functionally Graded NiTi, Journal of Alloys and Compounds, Vol. 851, 2021, pp. 156103.

[13] Meng, Q., Wu, Z., Bakhtiari, R., Shariat, B. S., Yang, H., Liu, Y., and Nam, T. H., A Unique "Fishtail-Like" Four-Way Shape Memory Effect of Compositionally Graded NiTi, Scripta Materialia, Vol. 127, 2017, pp. 84-87.

[14] Khan, M. I., Pulsed Nd: YAG Laser Processing of Nitinol, Ph.D. Dissertation, Mechanical and Mechatronics Engineering Dept., University of Waterloo, Waterloo, Ontario, Canada, 2011.

[15] Daly, M., Pequegnat, A., Zhou, Y. N., and Khan, M. I., Fabrication of a Novel Laser-Processed NiTi Shape Memory Microgripper with Enhanced Thermomechanical Functionality, Journal of Intelligent Material Systems and Structures, Vol. 24, No. 8, 2013, pp. 984-990.

[16] Panton, B., Zhou, Y. N., and Khan, M. I., A Stabilized, High Stress Self-Biasing Shape Memory Alloy Actuator, Smart Materials and Structures, Vol. 25, No. 9, 2016, pp. 095027.

[17] Zeng, Z., Oliveira, J. P., Ao, S., Zhang, W., Cui, J., Yan, S., and Peng, B., Fabrication and Characterization of a Novel Bionic Manipulator Using a Laser Processed NiTi Shape Memory Alloy, Optics and Laser Technology, Vol. 122, 2020, pp. 105876.

[18] Ge, F., Peng, B., Ke, W., Teshome, F. B., Du, X., and Zeng, Z., Design and Fabrication of Bionic Finger Driven by NiTi Shape Memory Alloys, Proceedings of the Eighth Asia International Symposium on Mechatronics, Springer Nature Singapore, Singapore, 2022, pp. 616-627.

[19] Khan, M. I., Zhou, Y., Effects of Local Phase Conversion on The Tensile Loading of Pulsed Nd: YAG Laser Processed Nitinol, Materials Science and Engineering: A, Vol. 527, No. 23, 2010, pp. 6235-6238.

[20] Michael, A., Pequegnat, A., Wang, J., Zhou, Y. N., and Khan, M. I., Corrosion Performance of Medical Grade NiTi After Laser Processing, Surface and Coatings Technology, Vol. 324, 2017, pp. 478-485.

[21] Mehrpouya, M., Gisario, A., Brotzu, A., and Natali, S., Laser Welding of NiTi Shape Memory Sheets Using a Diode Laser, Optics and Laser Technology, Vol. 108, 2018, pp. 142-149.

[22] Michael, A., Laser Processing and Modelling of Multiple Memory Shape Memory Alloys, Ph.D. Dissertation, Mechanical and Mechatronics Engineering Dept., University of Waterloo, Waterloo, Ontario, Canada, 2018.

[23] Panton, B., Laser Processing, Thermomechanical Processing, and Thermomechanical Fatigue of NiTi Shape Memory Alloys, Ph.D. Dissertation, Mechanical and Mechatronics Engineering Dept., University of Waterloo, Waterloo, Ontario, Canada, 2016.

[24] Pequegnat, A., Novel Laser Based NiTi Shape Memory Alloy Processing Protocol for Medical Device Applications, Ph.D. Dissertation, Mechanical and Mechatronics Engineering Dept., University of Waterloo, Waterloo, Ontario, Canada, 2014.

[25] Shamsolhodaei, A., Zhou, Y. N., and Michael, A., Enhancement of Mechanical and Functional Properties of Welded NiTi by Controlling Nickel Vapourisation, Science and Technology of Welding and Joining, Vol. 24, No. 8, 2019, pp. 706-712.

[26] Shamsolhodaei, A., Razmpoosh, M. H., Maletta, C., Magarò, P., and Zhou, Y. N., A Comprehensive Insight into The Superelasticity Measurement of Laser Welded NiTi Shape Memory Alloys, Materials Letters, Vol. 287, 2021, pp. 129310.

[27] Vâlsan, D. D., Bolocan, V. M., Novac, A., Chilnicean, G. A., and Crăciunescu, C. M., Analysis of Pulsed Laser Spot Effects on NiTi Wires, Solid State Phenomena, Vol. 332, 2022, pp. 59-66.

[28] Ge, F., Zeng, Z., Peng, B., Teshome, F. B., and Chen, L., Study on The Effect of Double-Sided Laser Welding of NiTi Shape Memory Alloys Wire, The International Journal of Advanced Manufacturing Technology, Vol. 120, No. 11-12, 2022, pp. 8201-8209.

[29] Amrollahipour, R., Kadkhodaei, M., Influence of Strain Rate on Stress–Strain Response of Ni–Mn–Ga Ferromagnetic Shape Memory Alloy Single Crystals, Iranian Journal of Science and Technology, Transactions of Mechanical Engineering, Vol. 41, 2017, pp. 265-268.

[30] Jamalimehr, A., Ravanbakhsh, H., Kadkhodaei, M., and Kamrani, M., Investigation of Dog-Bone Geometry for Simple Tensile Test of Pseudoelastic Shape Memory Alloys, Iranian Journal of Science and Technology, Transactions of Mechanical Engineering, Vol. 40, 2016, pp. 337-345.

[31] Brinson, L. C., One-Dimensional Constitutive Behavior of Shape Memory Alloys: Thermomechanical Derivation with Non-Constant Material Functions and Redefined Martensite Internal Variable, Journal of Intelligent Material Systems and Structures, Vol. 4, No. 2, 1993, pp. 229-242.

[32] He, X., Deb Roy, T., and Fuerschbach, P. W., Composition Change of Stainless Steel During Microjoining with Short Laser Pulse, Journal of Applied Physics, Vol. 96, No. 8, 2004, pp. 4547-4555.

[33] Jandaghi, M., Parvin, P., Torkamany, M. J., and Sabbaghzadeh, J., Alloying Element Losses in Pulsed Nd: YAG Laser Welding of Stainless Steel 316, Journal of Physics D: Applied Physics, Vol. 41, No. 23, 2008, pp. 235503.

[34] Sadiq, H., Wong, M. B., Al-Mahaidi, R., and Zhao, X. L., The Effects of Heat Treatment on The Recovery Stresses of Shape Memory Alloys, Smart Materials and Structures, Vol. 19, No. 3, 2010, pp. 035021.